TEMPERATURE-COMPENSATED PIEZOELECTRICALLY ACTUATED LAMÉ-MODE RESONATORS

Vikram Thakar[1] *and Mina Rais-Zadeh*[1]
[1]University of Michigan, Ann Arbor, USA

ABSTRACT

Electrostatically actuated Lamé-mode resonators are known to offer high quality factors (*Q*) in the low MHz frequency range [1], [2] but require large bias voltages and suffer from low power handling. In this work, we utilize piezoelectric transduction to circumvent the limitations of electrostatic actuation. Silicon dioxide refilled islands, used to achieve temperature compensation, are shown to provide a 20× improvement in the total charge pick-up, enabling piezoelectric actuation of Lamé-mode resonators. By optimizing the placement of the oxide-refilled islands and without changing the total oxide volume, the turnover temperature (TOT) can be designed to occur across a wide range from -40 °C to +120 °C without any significant *Q* degradation. Using such an approach multiple piezoelectric resonators with different TOTs can be fabricated on a single wafer, enabling multi-resonator systems stable across a wide temperature range.

INTRODUCTION

Low-power timing references are typically implemented using resonators operating at frequencies less than 100 MHz. From the considerations of phase noise, which translates into timing jitter, it is critical that the resonator has a high *Q*, large power handling limit, and low motional impedance. The isochoric mode shape of the Lamé mode of resonance enables low thermoelastic damping (TED) and thus a high device *Q* in the low MHz frequency regime [3] and electrostatically actuated Lamé-mode resonators have been demonstrated with *Qs* over a million at 6 MHz (Figure 1) [1], [4]. However, the relatively large bias voltage requirements and poor power handling capability makes it difficult to realize precision timing references with such electrostatically actuated resonators [5].

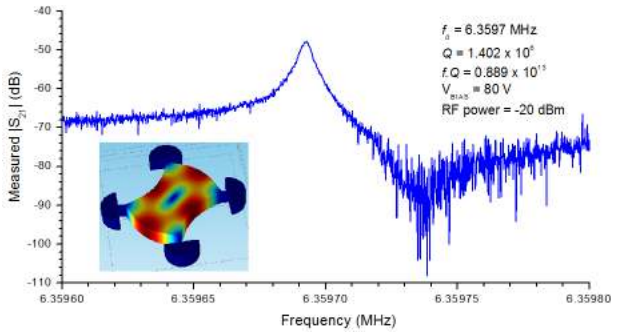

Figure 1: Measured frequency response of an electrostatically actuated Lamé-mode resonator showing a *Q* of 1.4 million. Inset shows the mode shape of the resonator.

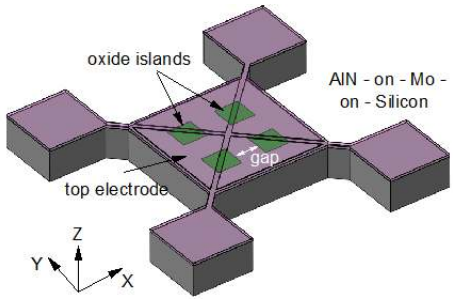

Figure 2: Schematic of a temperature-compensated Lamé-mode resonator. The location of the oxide-refilled trenches and the triangle shaped top electrode layout can be clearly seen.

Piezoelectric actuation obviates the DC bias requirements and ensures an improved power handling ability [6] and has been chosen as the transduction mechanism in this work. We compensate the temperature coefficient of frequency (TCF) of silicon using silicon dioxide refilled trenches positioned deliberately across the resonator body. Lamé-mode resonators actuated using piezoelectric transduction layer with Wurtzite symmetry (such as AlN and GaN) are susceptible to charge cancellation due to the equal magnitude and polarity of the d_{31} and d_{32} piezoelectric coefficients. We show that the presence of the oxide islands not only compensates the first-order TCF but also skews the strain profile across the resonator and provides a 20× improvement in the total charge pickup, enabling piezoelectric actuation of the Lamé-mode resonators.

RESONATOR DESIGN

Temperature Compensation

Silicon dioxide has been successfully used to overcome the large TCF of silicon [7]. The compensated composite resonators show a parabolic dependence of frequency with respect to the temperature with the overall frequency shift reduced to under 200 ppm across the industrial temperature range (as compared to ~3750 ppm for silicon only resonators) [7]. The TOT *i.e.* turnover temperature is defined as the inflection point of this parabola and determines the temperature at which the local TCF is zero.

For the compensation of bulk mode resonators, uniformly distributed oxide pillars have been used to limit the oxide thickness deposited [8]. In lieu of a uniform distribution of oxide, we utilize its location dependence on temperature compensation and place the oxide trenches around the resonator center, where strain energy is high [9], [10]. By careful control over the placement of these oxide-refilled trenches, it is possible to finely control the amount of compensation, which manifests as a change in the TOT

without increasing any processing steps. This enables the realization of multiple resonators with different TOTs and can enable multi-resonator systems that are temperature stable across the industrial temperature range.

Figure 2 shows a schematic of a piezoelectrically actuated Lamé-mode resonator with the location of the oxide-refilled trenches. The size of the resonator plate is 100 µm × 100 µm, while the four oxide-refilled islands are 20 µm × 20 µm each in size. The resonance frequency of the first order Lamé-mode can be approximately written as

$$f_{Lame} = \frac{1}{2L}\sqrt{\frac{E}{(1+\nu)\rho}}, \qquad (1)$$

where L is the side length of the resonator and E, ν and ρ are the effective Young's modulus, Poisson's ratio and density of the composite resonator, respectively. Assuming a temperature independent ν and ρ, the TCF of a composite Lamé-mode resonator can be written as

$$TCF = -\frac{1}{2}TCE - \alpha_L, \qquad (2)$$

where α_L is the coefficient of thermal expansion and TCE is the temperature coefficient of Young's modulus. Typically, the effective E of composite resonators is estimated by averaging the volumetric contribution of the different materials within the resonator. However, it has been shown that the effective E and consequently the TCE is not only a function of the volumetric composition but also of the location of the different materials within the resonator body [9]. Here, we show that a modified modeling framework considering the ratio of strain energy in oxide and silicon to that in the whole resonator can more accurately predict the temperature behavior of a composite resonator:

$$TCF_{resonator} = TCF_{Si} \times k + TCF_{ox} \times (1-k), \qquad (3)$$

where $\boldsymbol{k}$ is ratio of strain energy in silicon to that of the whole resonator. Figure 3 (inset) shows the simulated strain energy gradient across a Lamé-mode resonator. From the energy distribution, it can be inferred that when the oxide islands are placed closer to the center their total strain energy content is significantly higher than when they are placed far away from the center. Figure 3 shows the comparison between the simulated TOT with the one analytically estimated using (3). For the analytical estimation, the magnitude of strain energy in the oxide and silicon is required. Table 1 summarizes the strain energy values taken from simulations and Table 2 details the material parameters used in the simulations.

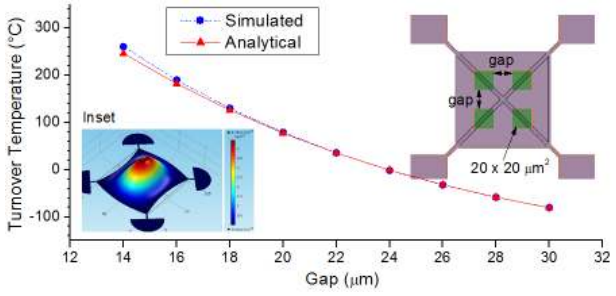

Figure 3: Comparison of the simulated and analytically estimated turnover temperature for the compensated Lamé-mode resonators. (Right) Top view showing the "gap" and location of the oxide-refilled islands. (Inset) Simulated strain energy across the resonator for the Lamé-mode shape. The gradient of energy, which is maximum at the center to its minima around the device edge, can be clearly seen.

Table 1: Simulated strain energy in silicon (E_{si}), total strain energy (E_{total}) and the calculated k. Gap is defined in Figure 3.

gap	14	16	18	20	22	24	26	28	30
E_{si} ($\times 10^{12}$)	1.116	1.19	1.247	1.291	1.353	1.385	1.433	1.485	1.491
E_{total} ($\times 10^{12}$)	1.676	1.731	1.764	1.78	1.824	1.829	1.859	1.897	1.879
k	0.666	0.687	0.707	0.725	0.742	0.757	0.771	0.783	0.793

Table 2: Material properties used in the estimation of the TOT using FEM and analytical formulation using (3).

Parameter	Silicon	Oxide	Unit
Young's modulus	169	71	GPa
First-order TCE	-64	187.5	ppm/K
Second-order TCE	-75	40	ppb/K^2

Piezoelectric actuation

As pointed out earlier, the crystal symmetry of AlN makes it challenging to actuate the fundamental Lamé-mode of resonance. Each point in the resonator undergoes similar expansion and contraction in the two in-plane orthogonal directions. Since the d_{31} and d_{32} piezoelectric coefficients of AlN have the same magnitude and polarity, the net piezoelectric charge pick up is very small. The presence of the oxide islands within the resonator volume skews the strain profile in the resonator and the temperature compensation strategy has an added benefit of improving the total charge pickup and helps improve the insertion loss of the resonator. Figure 4 plots the net strain across (a) an uncompensated and (b) a compensated Lamé-mode resonator across the AlN surface and clearly highlights the effect of including the oxide islands. To estimate the improvement in charge pickup of compensated resonator (compared to the uncompensated one), the strain gradient is integrated across the AlN layer and the results are summarized in Table 3. A 20× improvement in the total strain is seen due to the inclusion of oxide islands.

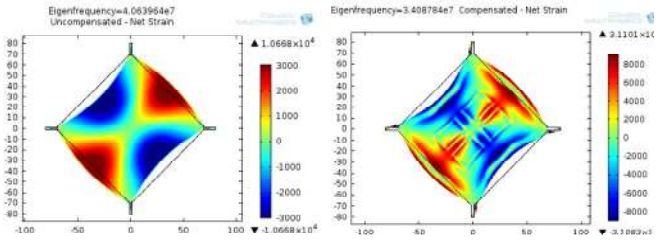

Figure 4: Net strain across the AlN surface for (a) uncompensated and (b) compensated Lamé-mode resonator. The presence of the oxide islands is seen to skew the strain profile. The color gradient plots the change in net strain across the surface, with red and blue representing positive and negative strains respectively.

Table 3: Estimated volume integral of strain in the AlN layer along the resonator in-plane axes showing the effect of silicon and oxide-refilled trenches on the effective charge pick-up.

Resonator	Strain in X (ε_X) (m^3)	Strain in Y (ε_Y) (m^3)	$\varepsilon_X - \varepsilon_Y$ (m^3)
AlN	3.95×10^{-15}	3.96×10^{-15}	2.51×10^{-18}
AlN-on-Si	4.03×10^{-15}	4.10×10^{-15}	6.74×10^{-17}
AlN-on-Si with oxide	2.03×10^{-15}	0.662×10^{-15}	1.37×10^{-15}

Based on the observed strain profile, four triangular shaped electrodes with the diametrically opposite electrodes connected together are used to achieve piezoelectric actuation. Figure 5 shows the simulated frequency response of a compensated and uncompensated resonator which highlights the improvement in insertion loss seen due to the presence of the oxide islands.

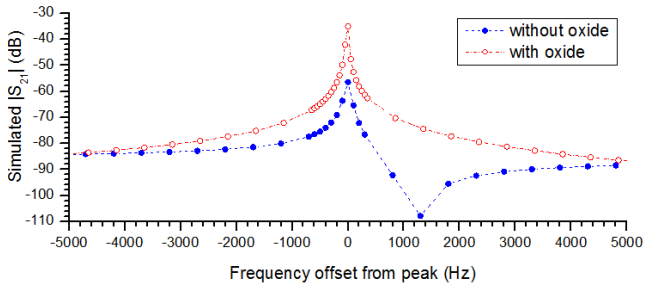

Figure 5: Simulated $|S_{21}|$ for a temperature compensated (with oxide) and uncompensated (without oxide) Lamé-mode resonator.

Tether Optimization for reduced Anchor dissipation

While Lamé-modes do not suffer from TED, they have been shown to be susceptible to anchor Q degradation [1]. The increased anchor dissipation has been shown to be caused by the flexural resonance modes of the tether, when matched to the frequency of the Lamé-mode [1]. With the inclusion of the oxide islands, the frequency of the fundamental Lamé-mode is seen to decrease (for a given resonator side length) and thus changes the optimum tether geometry. Using the approach presented in [1], the support tethers of the temperature-compensated Lamé-mode resonator are optimized to have a tether length of 10.5 µm and tether width of 2 µm.

FABRICATION

Devices are fabricated on a silicon-on-insulator (SOI) wafer with a 25 µm thick high-resistivity (>1000 Ω.cm) device layer. Figure 6 shows the schematic of the fabrication process and is similar to the one used in [9]. In order to obtain completely refilled trenches, the trench DRIE is optimized to provide a straight sidewall with an opening of 1.2 µm. The spacing between the trenches is set to be 0.8 µm. Figure 7 shows cross-section SEM images of the DRIE trenches and oxide-refilled islands. Figure 8 shows an SEM image of a fabricated Lamé-mode resonator.

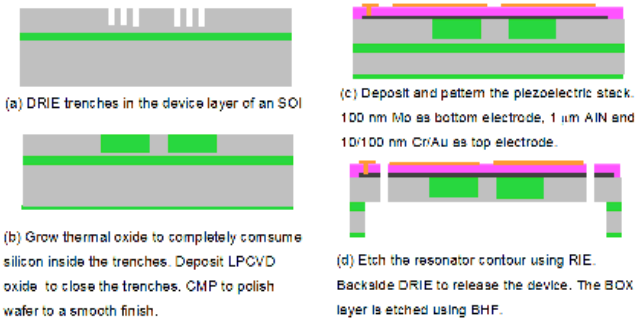

Figure 6: Process flow used for the fabrication of temperature-compensated piezoelectrically actuated Lamé-mode resonators.

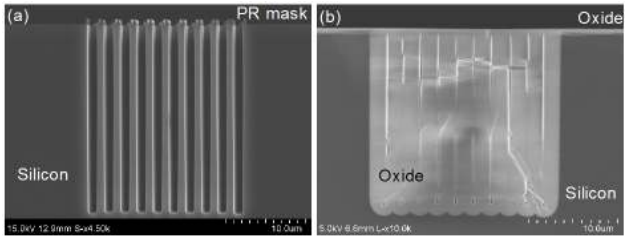

Figure 7: Cross-section SEM images of (a) the DRIE trenches to be oxidized, (b) an oxide-refilled island.

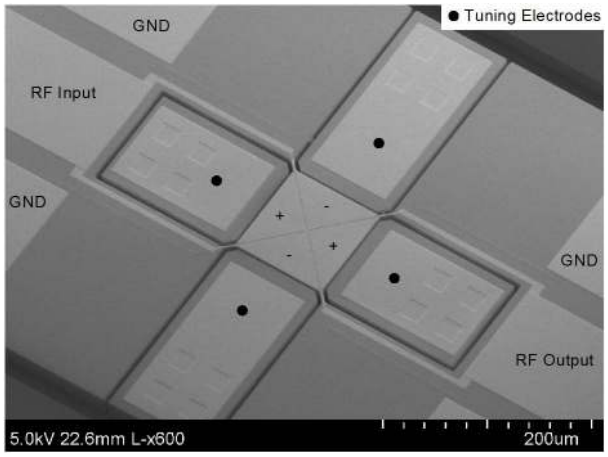

Figure 8: A SEM image of a fabricated Lamé-mode resonator. The top input and output ports are labeled with '+' and '-', respectively and resembles the net strain profile seen in Figure 4. The oxide-refilled trenches are embedded within the silicon body and are not visible through the AlN layer.

MEASURED RESULTS

In order to characterize the performance of the resonators, on wafer measurements are carried out in a temperature-controlled probe station at a pressure of ~100 µTorr. Figure 9 (a) and (b) plot the measured frequency response of a temperature-compensated and uncompensated piezoelectrically-actuated Lamé-mode resonator, respectively. As predicted, the insertion loss of the compensated resonator is lower and the signal to noise ratio is higher than the resonator without the compensating trenches. Also, note that the Qs of the two resonators are comparable.

Figure 10 shows the measured frequency shift with temperature for three temperature-compensated Lamé-mode resonators. The three resonators have the same volume of oxide but different "gap" between the oxide islands. The measured results in Figure 10 compare well with the estimated TOT presented in Figure 3. There is a nominal TOT shift of approximately -80 °C for all designs which can be attributed to the piezoelectric stack. The TOT estimates given in Figure 3 ignore the presence of the bottom electrode, AlN, and the top electrode layers.

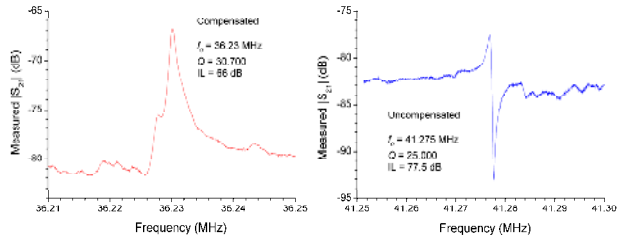

Figure 9: Measured frequency response of a (left) temperature compensated and (right) uncompensated Lamé-mode resonator, measured at room temperature and in vacuum.

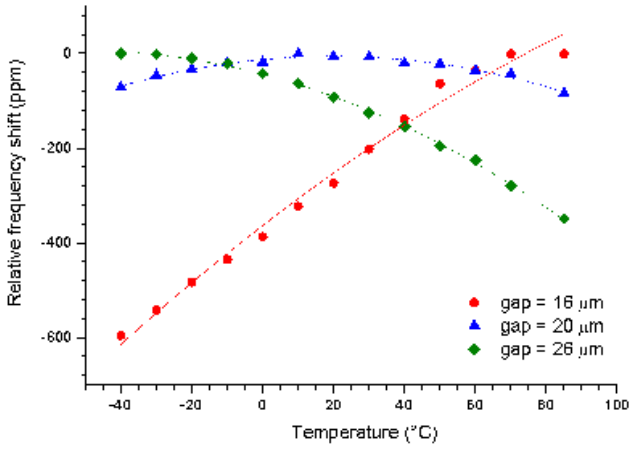

Figure 10: Measured peak frequency shift as a function of temperature for three different "gaps" between the oxide islands.

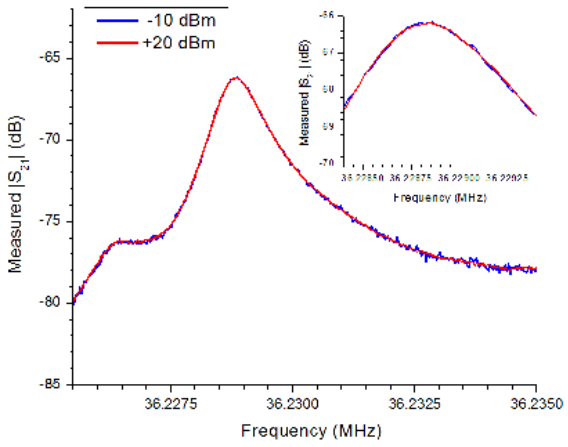

Figure 11: Measured frequency response of a Lamé-mode resonator at input RF power of -10 dBm and +20 dBm, showing no non-linearity in the response.

Figure 11 shows the measured frequency response of the compensated device shown in Figure 9(left) at -10 dBm and +20 dBm of input RF power. No non-linear behavior is visible, indicating the high power handling capability of these resonators.

CONCLUSIONS

Through the inclusion of oxide islands within the resonator volume, we achieved complete cancellation of the first-order TCF and demonstrated the ability to tune the turnover temperature through placement of the oxide islands within the resonator. The presence of the oxide islands was shown to improve the charge pickup by 20× and enabled piezoelectric actuation of temperature-compensated Lamé-mode resonators. Using this approach three compensated resonators with different TOT were demonstrated. Such resonators can be utilized in a multi-resonator system to improve the temperature stability of timing references across the entire industrial temperature range.

ACKNOWLEDGEMENTS

The authors acknowledge staff at the Lurie Nanofabrication Facility, a member of NSF NNIN, for their help with device fabrication. This work is supported by NASA under the Chip-Scale Precision Timing Unit project (Grant #NNX12AQ41G).

REFERENCES

[1] V. Thakar and M. Rais-Zadeh, "Optimization of tether geometry to achieve low anchor loss in Lamé-mode resonators," *IFCS '13*, Prague, CZ, July, 2013.

[2] J. Lee, J. Yan and A. Seshia, "Study of lateral mode SOI-MEMS resonators for reduced anchor loss," *J. Micromech. Microeng.*, vol. 21, pp. 045010, 2011.

[3] S. Chandorkar, *et al.*, "Limits of quality factor in bulk-mode micromechanical resonators," *MEMS 2008*, Jan. 2008.

[4] L Khine and M. Palaniapan, "High-Q bulk-mode SOI square resonators with straight-beam anchors," *J. Micromech. Microeng.*, vol. 19, pp. 015017, 2009.

[5] Y. Xu and J. E.-Y. Lee, "Mechanically coupled SOI Lamé-mode resonator-arrays: synchronized oscillations with high Q factors of 1 million," *IFCS 2013*, Prague, CZ, 21-25 Jul 2013.

[6] Z. Wu, A. Peczalski, V. Thakar, and M. Rais-Zadeh, "A low phase-noise Pierce oscillator using a piezoelectric-on-silica micromechanical resonator," *Transducers '13*, June, 2013.

[7] R. Melamud, *et al.*, "Temperature-compensated high-stability silicon resonators," *Appl. Phys. Lett.*, vol. 90, no. 24, pp. 244107, Jun. 2007.

[8] R. Tabrizian, G. Casinovi and F. Ayazi, "Temperature-stable high-*Q* AlN-on-silicon resonators with embedded array of oxide pillars," *Hilton Head '10*, Hilton Head Island, SC, pp. 100-101, June 2010.

[9] V. Thakar, Z. Wu, A. Peczalski, and M. Rais-Zadeh, "Piezoelectrically transduced temperature-compensated flexural-mode silicon resonators," *JMEMS*, Vol. 22, No. 3, pp. 819-823, 2013.

[10] M. Allah, *et al.*, "Temperature compensated solidly mounted bulk acoustic wave resonators with optimum piezoelectric coupling coefficient," *IEDM '09*, pp. 1-4, 7-9 Dec. 2009.

CONTACT

Vikram Thakar, tel: +1-734-3443480; thakar@umich.edu
M. Rais-Zadeh, tel: +1-734-7644249; minar@umich.edu